Towards a Broadband and Squint-Free K_u-Band Phased Array Antenna System for Airborne Satellite Communications

D. Marpaung[1], L. Zhuang[1], M. Burla[1], C. Roeloffzen[1], J. Verpoorte[2], H. Schippers[2], A. Hulzinga[2], P. Jorna[2], W. P. Beeker[3], A. Leinse[3], R. Heideman[3], B. Noharet[4], Q. Wang[4], B. Sanadgol[5], and R. Baggen[5]

[1]*University of Twente, PO Box 217, 7500 AE, Enschede, the Netherlands*
{d.a.i.marpaung, l.zhuang, m.burla, c.g.h.roeloffzen}@ewi.utwente.nl

[2]*National Aerospace Laboratory (NLR), Anthony Fokkerweg 2, 1006 BM Amsterdam, the Netherlands*
{jaco.verpoorte, harmen.schippers, adriaan.hulzinga, pieter.jorna}@nlr.nl

[3]*LioniX B.V., PO Box 456, 7500 AL, Enschede, the Netherlands*
{w.p.beeker, a.leinse, r.g.heideman}@lionixbv.nl

[4]*Acreo AB, Electrum 236, SE-164 40, Kista, Sweden*
{bertrand.noharet, qin.wang}@acreo.se

[5]*Department of Antennas & EM Modeling, IMST GmbH, Carl-Friedrich-Gauß Str. 2-4, 47475 Kamp-Lintfort, Germany*
{bahram, baggen}@imst.de

Abstract— **In this paper, we describe the design and the development of a K_u-band phased array antenna system for the reception of a digital video broadcasting by satellite (DVB-S) signal. A concept of optical beamforming is implemented to provide a squint-free beam steering over the entire Ku-band (10.7-12.75 GHz) as well as to achieve seamless tunability of the beam pointing direction. The total antenna system is described and the system performance is simulated. Requirements for system components are formulated and the development of these components towards the implementation of the broadband, squint-free phased array antenna system is reported.**

I. Introduction

Novel avionic communication systems are required for various purposes, for example to increase the flight safety and operational integrity as well as to enhance the quality of service to passengers on board. To serve these purposes, a key technology that is essential to be developed is an antenna system that can provide broadband connectivity within aircraft cabins at an affordable price. Currently, in the European Commission (EC) 7th Framework Programme SANDRA project, a development of such an antenna system is being carried out. The system is an electronically-steered phased-array antenna that has a low aerodynamic profile. The reception of digital video broadcasting by satellite (DVB-S) signal which is in the frequency range of 10.7-12.75 GHz (K_u-band) is being considered. The desired antenna should be able to receive the entire DVB-S band at once without beam-squint and should comply with the requirements of the DVB-S system [1].

In this work, we describe the design and the development of the phased array antenna system that complies with the aforementioned requirements. A concept of optical beamforming [1, 2] is implemented to provide a squint-free beam over the entire Ku-band for all the desired pointing directions. Additionally, seamless tunability of the beam pointing direction is achieved with this concept by using continuously tunable optical delays. In this paper the total antenna system is described and the system performance is simulated. Requirements of system components are thus formulated and the development of these components towards the broadband, squint-free phased array antenna system is reported.

The remainder of this paper is organized as follows: in Section II the PAA system architecture is described. The system modelling and performance analysis is presented in the third section. In Section IV the current status of the development of the components in the system is reported. The paper closes with conclusions in the final section.

II. System Architecture

The schematic of the phased-array antenna (PAA) system considered in this work is shown in Fig.1. As a basic building block, we consider an antenna tile (an 8×8 module) consisting of 64 antenna elements (AEs), as shown in Fig. 1A. Since the received signal power density from the satellite is relatively low, the antenna should have a high gain and low noise temperature to achieve the required carrier-to-noise ratio (CNR). This dictates a number of antenna elements (AEs) of at least 1800 [1]. To meet the requirements, the tiles are arranged to assemble a PAA consisting of 2048 AEs (a power of 2) as shown in Fig. 1B. The antenna elements are stacked patch antennas that are impedance matched between 10.7 and 12.75 GHz [3]. To delay and combine (i.e. to beamform) the signals received by the AEs, a hybrid combination of monolithic microwave integrated circuit (MMIC) beamforming and optical beamforming is proposed. In this hybrid configuration, a chain of low noise amplifier (LNA) and MMIC tunable phase shifter follows each AE. Using these

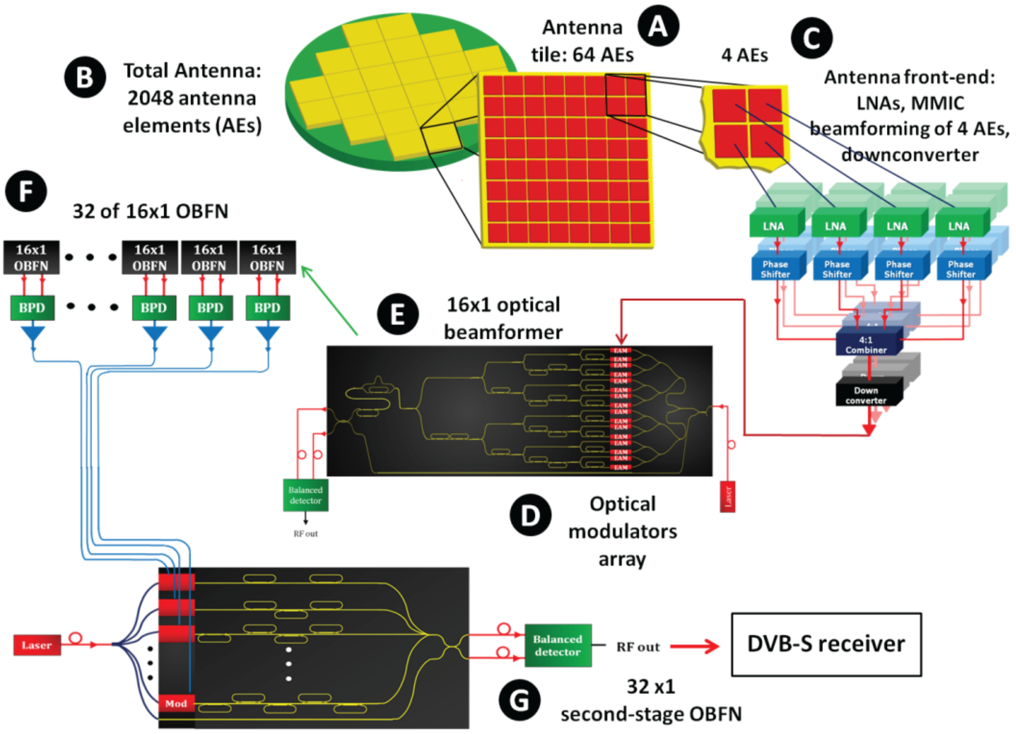

Fig. 1. The phased-array antenna system considered in this work. (A) An antenna tile consisting of 64 elements, (B) the total antenna system with >1800 AEs, (C) the RF front-end consisting of LNAs, MMIC phase shifter, a 4-to-1 combiner and a downconverter, (D) an array of electroabsorption modulator integrated with a 16×1 optical beamformer (E). The RF outputs of 32 of these 16×1 beamformer (F) are combined by a second stage optical beamfomer with 32 inputs and one output (G)

phase shifters and a combiner, the MMIC beamforming is applied to a sub-array consisting of 4 neighbouring AEs. The output signal from the combiner is then down-converted to the L-band (Fig. 1C). To combine the output signals from the front–ends an optical beamforming scheme is used. The optical beamformers considered here are based on cascaded optical ring resonators (ORRs) [1, 2]. These ORRs are used to generate continuously tunable true time delays (TTDs) within the desired band. Since TTD elements are used instead of (frequency-dependent) phase-shifters, squint-free operation can be achieved. Moreover, since the generated TTDs are continuously tunable, seamless tuning of the beam pointing direction can be achieved with this system. The detailed principle of these optical beamformers has been well documented in [1, 2].

The signals from the front ends of each tile are then fed to an array of 16 electroabsorption modulators (EAMs), to convert these signals to the optical domain (Fig. 1D). Each modulator array will interface with a 16×1 optical beamforming network (OBFN) (Fig. 1E). In previous investigations, it was demonstrated that a two-level OBFN architecture is the most feasible way to handle the large number of AEs [1]. Thus, a larger OBFN with 32 input ports is used at the second-level to combine the outputs of 32 16×1-OBFNs in the first stage (Fig. 1F and 1G). In the following section, the performance analysis of the system described above is presented.

III. System Performance Analysis

A system level simulation has been developed to determine the required performance of the system components. The K_u-band antenna should receive signals from satellites, with a power level in the order of -150 dBW per transponder. Taking into account the fluctuating atmospheric conditions and changing of location, we set the requirement of the minimum detectable received power 10 dB lower to -160 dBW. Moreover, a maximum 2D scan angle of $\pm 60^o$, an antenna gain in the order of 35 dBi and a sky noise temperature of 50 K have been assumed. As a figure of merit, the minimum CNR per-channel required at the input of the DVB-S receiver is set at 8 dB, in a transponder bandwidth of 33 MHz [1].

In the analysis presented here the complex system in Fig.1 is simplified to a two-port cascaded system. The procedure of this simplification is reported in [1]. The resulting two-port models with its relevant parameters are depicted in Fig. 2.

Using the input antenna parameters described above and using the 8 dB CNR as a target value, the performance of the simplified system in Fig.2 is simulated. The aim is to determine several important properties of the system components namely the front-end, the optical modulators and the optical beamformer chip. For the front-end, an emphasis is placed on the gain and the noise figure. The efficiency of the optical modulators to convert RF signals

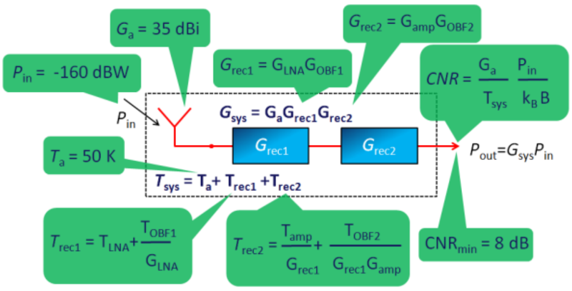

Fig. 2. Simplified two-port model of the PAA system in Fig.1

to modulated optical signals is found to be paramount to ensure the signal quality at the output.

Two important parameters of that signify the modulator efficiency, namely, the optical insertion loss and the equivalent half-wave voltage are defined and their optimum values are determined. As for the optical beamformer chip the most important parameter is the optical waveguide propagation loss, expressed in dB/cm.

In Fig. 3 the gain and noise figure requirements for the front-end can be deduced. Without loss of generality, here the front-end has been modelled as a single LNA. The graph depicts the maximum noise figure of the front-end to still achieve the minimum CNR of 8 dB for various gain of the LNA. This is depicted as a function of the received power per transponder. It has been assumed here that the system uses a laser with a 100 mW power and a RIN of -150 dB/Hz, a balanced detector with a responsivity of 0.8 A/W, an optical modulator with an insertion loss of 2 dB and a half-wave voltage of 1 V and optical beamformers with a waveguide propagation loss of 0.2 dB/cm.

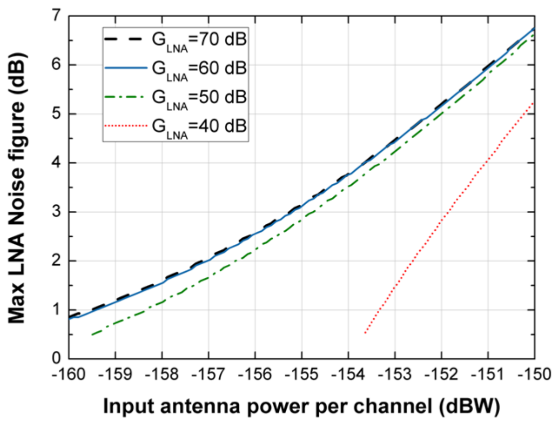

Fig. 3. The maximum noise figure of the front-end to achieve 8 dB CNR for various gain of the front end depicted as a function of the received power per transponder

From the figure above one can determine that in order to achieve the required CNR with a received power of -160 dBW, the front end gain should be > 60 dB and NF < 1 dB. Since this is very challenging to achieve, the system requirement aimed in this work is slightly relaxed such that a power margin of 6 dB (input power of -156 dBW) is sufficient. Thus in this case, the NF requirement of the front-end is relaxed to < 2.5 dB for gain of >60 dB. These will be the target values for the front-end design.

In Fig. 4 the CNR is depicted as function of the optical waveguide loss in dB/cm. Note that here again a 10 dB power margin has been assumed. Three situations have been considered. First, the LNA gain and the modulator half-wave voltage (V_π) are set at 70 dB and 1.0 V, respectively. With these parameters, the 8 dB CNR can be met for all waveguide loss values from 0 to 0.5 dB/cm (solid curve). But if the V_π increases, for example to 4.0 V, the specified CNR can only be met with a waveguide loss of less than 0.2 dB/cm (dashed-curve). The graph depicts the importance of achieving low waveguide loss, high LNA gain and low modulator V_π.

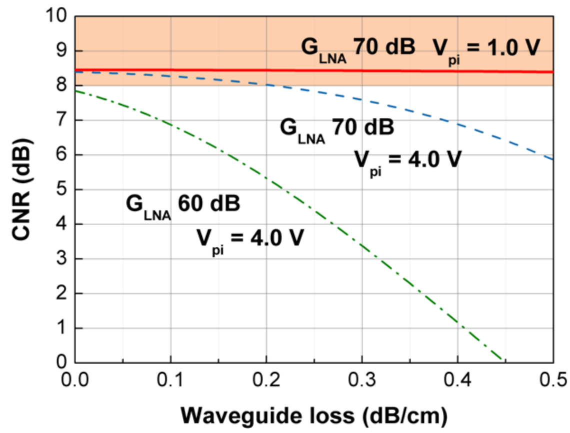

Fig. 4. The simulated system CNR as a function of the waveguide propagation loss

Since the development of the modulators is still in the early stage, preliminary requirements of insertion loss < 3 dB and $V_\pi < 4$ V has been considered.

IV. Development of the System Components

From the system level simulation the required characteristics of each component of the system are specified. In the current phase of the SANDRA project numerous efforts have been directed towards meeting the specified performance. The development of three main parts of the system, namely the front ends (LNAs, phase shifters and downconverter chips), the optical modulators and the optical beamformer are described below.

A. Front End

The projected configuration of the front-end is depicted in Fig. 5a. Here, the output signal of 4 AEs will be amplified, combined and subsequently downconverted to the L-band (950-2150 MHz). The target values of gain and noise figure for the complete chain have been set to 70 dB and 2.0-2.5 dB, respectively. From the front-end design point of view, downconversion to the L-band is advantageous to avoid oscillations due to the large amplification. The oscillations can be minimized by means of distributing the gain at the two frequency bands.

Due to size constraints it is desirable to use MMICs with a high degree of integration. For this reason the so-called *corechips* will be used in the design. These are MMIC-building blocks that integrate different functionalities in the same chip. Here, the combined functionalities of amplification (LNA) and phase shifting are desired. The one selected for this design is a corechip that was previously designed for the NATALIA-project [4] and manufactured by the foundry OMMIC. It consists of a two-stage LNA, 4 bit phase shifter and digital logic. The projected gain and NF of the corechip are 12 dB and 1.7 dB, respectively, with an assumption that the coupling loss from the antenna to the chip is less than 0.5 dB.

The outputs of the four corechips are subsequently combined in a 4:1 combiner followed by an LNA. The down-conversion is performed after combining the 2×2 sub array. The proposed chip for down-conversion here is manufactured by NXP. This chip is a highly integrated IC that includes an LNA, a mixer, a down-converter, a PLL, a crystal oscillator, and an IF buffer. This chip supports RF input frequencies between 10.7 and 12.75 GHz, and uses a selectable LO that operates at 9.75 or 10.6 GHz. Finally an L-band amplifier is placed after the downconverter to achieve the gain in the L-band. The preliminary front-end layout of a 2×2 sub-array is depicted in Fig. 5b.

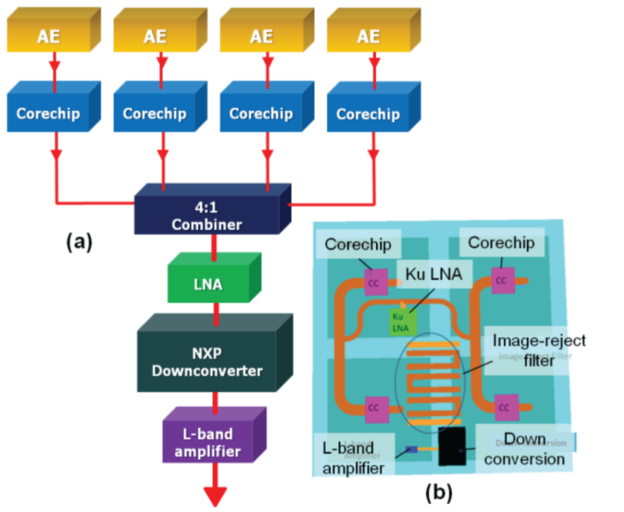

Fig. 5. (a) The configuration of the front-end. The corechip consists of an LNA and a 4-bit phase shifter. The NXP chip is used for downconversion and amplification. (b) Schematic layout of the RF front-end

The overview of the projected gain and noise figure of the complete front-end chain is summarized in Table I. A gain of 70 dB and a noise figure of 2.4 dB are feasible.

B. Optical Modulators

The optical modulators developed in this work are surface-normal electroabsorption modulators (EAMs) based on InGaAs/InAlAs coupled quantum wells [5]. The structure of the modulator is shown in Fig. 6a. For test purposes, the modulator is mounted on a PCB using wire bonds.

TABLE I
OVERVIEW OF GAIN AND NOISE FIGURE OF THE FRONT-END

OVERVIEW OF GAIN AND NF			
Element	**Gain**	**NF**	**Components functionality**
Corechip	12	1.7	Amplification and Phase Shifting
4-to-1 Combiner	-1	1	Constructing a 2x2 Subgroup
Ku LNA	13	2	Second Stage Amplification
Image Filter	-3	2	Rejecting Image Frequencies
NXP Chip	35	9	Down-conversion and Amplification in Ku and L band
L-band Amplifier	14	4	Gain Compensation in L band
Total System	***70***	***2.4***	

An SMA connector is then soldered to the PCB to supply the required reverse bias voltage and the RF signal (Fig. 6b). Although so far tests have been conducted on the individual modulators, the proper system operation requires an optical modulator array (Fig. 6c) to be developed.

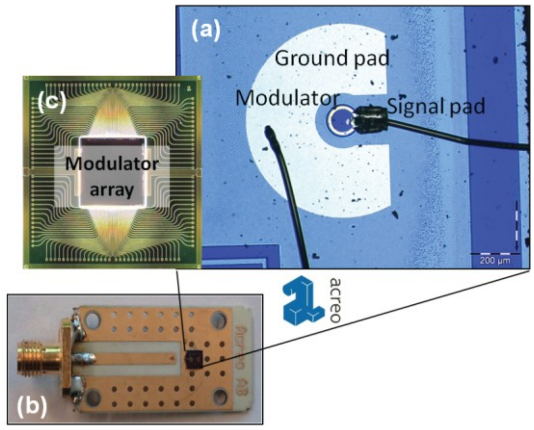

Fig. 6. Surface-normal electroabsorption modulators developed in this work. (a) The modulator structure, (b) an individual modulator mounted on a PCB, and (c) modulator array

As mentioned in the previous section, the modulators need to fulfil the specification with respect to their modulation speed (RF bandwidth), insertion loss and RF half-wave voltage (V_π) that describes the modulator sensitivity. The modulator speed depends on the size of the modulator. For a rough estimation of its bandwidth, the modulator can be modelled as an RC circuit where the capacitance depends linearly on the aperture area of the modulator. Thus, the smaller the modulator aperture, the higher cut-off frequency will be. For a relatively small EAM with an aperture diameter of 25 µm, the 3 dB cut-off frequency is expected to be in the order of 12 GHz. This is well above the intended frequency range of operation in the L-band resulting from the downconversion in the front-end.

To verify the modulator bandwidth, a measurement on the modulator frequency response (s_{21}) is carried out. Here the device under consideration is a reflective EAM with an aperture size of 25 µm. The measurement result for various reverse-bias voltages is depicted in Fig. 7. Here, a laser with an optical wavelength of 1530 nm and an optical power of +9 dBm has been used as the optical source. It can be seen from the figure that in an extended frequency range of operation (1-5 GHz, marked as the shaded area in Fig. 7) the modulator shows a relatively flat frequency response, with a 6 dB bandwidth of 5 GHz for a reverse bias of -3 V and -5 V.

It is important to point out from Fig. 7 that the magnitude of the frequency response is relatively low (approximately -45 dB). The origin of this large RF-to-RF loss is still under investigation. Currently a lot of efforts are towards the improvement of the design and the quality of the wirebonds and the RF PCB used to mount the modulator. These improvements expectedly will lead to an accurate determination of the modulator V_π

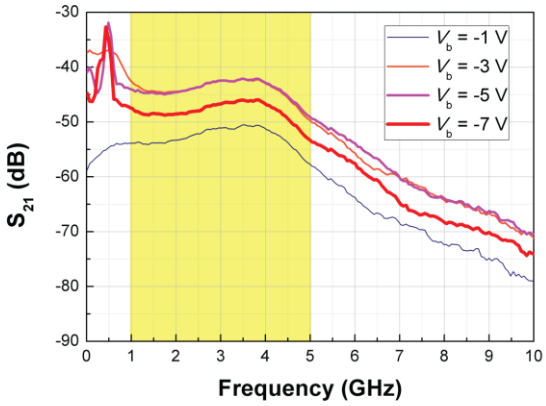

Fig. 7. The measured frequency response (s_{21}) of a reflective electroabsorption modulator with a 25 µm aperture for various reverse-bias voltages. The optical wavelength of the laser is 1530 nm

C. *Optical Waveguide Technology*

As mentioned in the previous section, the required value for the waveguide propagation loss is equal to or lower than 0.2 dB/cm at the optical wavelength of 1550 nm. In order to achieve this various test structures have been developed in the novel TriPleX waveguide technology [6]. With a novel type of waveguide structure the propagation loss target is 0.05 dB/cm.

A propagation loss measurement was performed in an optical ring resonator structure using the method reported in [7]. A propagation loss as low as 0.2 dB/cm for TE polarized light has indeed been achieved as shown in the measurement result in Fig. 8. This measurement was performed on a waveguide with the width of 1.3 µm. The bend radius of 125 µm was chosen to ensure that the measured loss is dominated by the waveguide loss instead of the bend loss. Thus, from this result it is confirmed that the required value for the propagation loss has been met.

Furthermore, from the simulation results it is expected that the bend loss will not become the dominant factor for a bending radius as low as 75 µm. It is important to mention that at these small bending radii a dramatic reduction of the optical beamformer chip size can be realized, which is nearly 10 times smaller compared to the existing chip reported in [2].

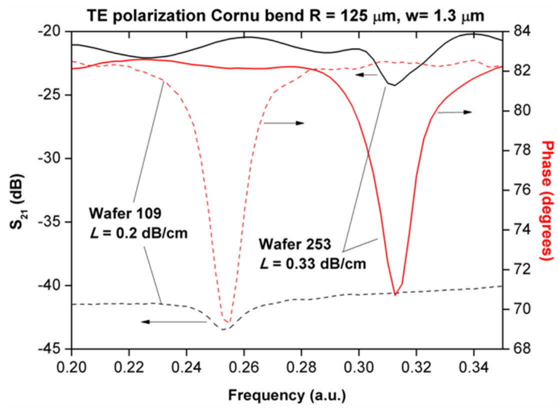

Fig. 8. Result of the propagation loss characterization of an optical ring resonator. A very low loss of 0.2 dB/cm has been achieved

V. Conclusions

We have reported the design, performance analysis and the progress on components development of a novel phased-array antenna system for airborne applications. A system level simulation has been used to determine the target values for the key parameters of the system components. Various targets like the front-end gain and noise figure as well as the propagation loss of the optical waveguide have been met. Further investigation on the performance of the optical modulator and the realization of the entire system is underway.

Acknowledgment

The research described in this paper is funded by the European Commission in the 7th Framework Program. The SANDRA project is a Large Scale Integrating Project for the FP7 Topic AAT.2008.4.4.2 (Integrated approach to network centric aircraft communications for global aircraft operations).

References

[1] A. Meijerink et al., “Novel ring resonator-based integrated photonic beamfomer for broadband phased-array receive antennas – part I: design and performance analysis”, Journal Lightwave Technol., Vol. 28, No.1, pp. 3-18, Jan. 2010.

[2] L. Zhuang et al., “Novel ring resonator-based integrated photonic beamfomer for broadband phased-array receive antennas – part II: experimental prototype”, Journal Lightwave Technol., Vol. 28, No.1, pp. 19-31, Jan. 2010.

[3] H. Schippers et al., “Broadband Optical Beamforming for Airborne Phased Array Antenna”, Proc. of the IEEE Aerospace Conference, Big Sky, Montana, USA, March 2009.

[4] R. Baggen et al., “First Prototyping of a Compact Mobile Ku-Band Satellite Terminal”, Proc. of the Fourth European Conference on Antennas and Propagation (EuCAP 2010), pp.1-4, 12-16 April 2010.

[5] Q. Wang et al., “1550 nm transmissive/ reflective surface-normal electro-absorption modulator arrays”, Electron. Lett. Volume 42, Issue 1, pp. 47–49, 2006.

[6] R.G. Heideman et al., "Large-Scale Integrated Optics Using TriPleX Waveguide Technology: From UV to IR", Proc. SPIE 7221, pp. 72210R-1-72210R-15, 2009.

[7] C. G. H. Roeloffzen et al., “Ring resonator-based tunable optical delay line in LPCVD waveguide technology,” in Proc. IEEE/LEOS Benelux Chapter, 10th Symp., pp. 71–74, 2005.